

Spatio-Temporal Road Detection from Aerial Imagery using CNNs

Belén Luque¹, Josep Ramon Morros², Javier Ruiz-Hidalgo³

Signal Theory and Communications Department

Universitat Politècnica de Catalunya - BarcelonaTech, Spain

¹luquelopez.belen@gmail.com, {²ramon.morros, ³j.ruiz}@upc.edu

Keywords: Computer vision, Road detection, Segmentation, Drones, Neural networks, CNNs.

Abstract: The main goal of this paper is to detect roads from aerial imagery recorded by drones. To achieve this, we propose a modification of SegNet, a deep fully convolutional neural network for image segmentation. In order to train this neural network, we have put together a database containing videos of roads from the point of view of a small commercial drone. Additionally, we have developed an image annotation tool based on the watershed technique, in order to perform a semi-automatic labeling of the videos in this database. The experimental results using our modified version of SegNet show a big improvement on the performance of the neural network when using aerial imagery, obtaining over 90% accuracy.

1 INTRODUCTION

Even though drones were initially developed for military purposes, they have become surprisingly popular for civilian and business use in the past few years. It is fairly easy to attach a camera to a drone, which allows for a large amount of applications. For instance, they are used as a support system in firefighting activities, as a drone can provide a map of the fire's progress without endangering any human life. Drones are also used for traffic analysis and exploring hard-to-access areas, where they can provide more mobility than other technologies. In order to analyze and process the images captured by a drone, it is necessary to use computer vision techniques. However, the nature of these images raises difficulties, as they present an outdoor location with a complex background. The camera is in motion, so the background obtained is not static, but changes from frame to frame. Furthermore, the perspective of a given object can vary widely depending on the position of the drone in relation to the ground.

The main goal of this work is detecting a road from the point of view of a drone, which is necessary - or very helpful - in a lot of applications, like the ones mentioned above. The segmentation of the images is carried out using SegNet (Badrinarayanan et al., 2015), a deep fully convolutional neural network architecture for semantic pixel-wise segmentation, originally trained to segment an image in 11 classes (sky,

building, pole, road, pavement, tree, sign symbol, fence, car, pedestrian and bicyclist). However, the images used for the original training of SegNet are taken from a car driver's point of view. This leads to a poor performance of SegNet when using aerial imagery, so we have modified and retrained the system with a new database and diminished the classes from 11 to 3 (*road*, *sky* and *other*). We created this new database by gathering existing videos from different sources. As these videos were unlabelled, we have also developed a semi-automatic labelling tool to obtain the necessary ground truth to train a neural network. Moreover, there is a certain correspondence between consecutive frames in a video that we use after the segmentation with SegNet to improve the result, which becomes more consistent and robust. Figure 1 shows the block diagram of the flow used in this work.

This paper is organized as follows: In section 2, we do a brief review of some state-of-the-art techniques for road detection. Next, we explain our method for doing so in section 3, where we detail both the image segmentation and the temporal processing blocks. Afterwards, section 4 describes the creation and labelling of our new database. Finally, we show the results we have obtained in section 5, before our conclusions in the last section.

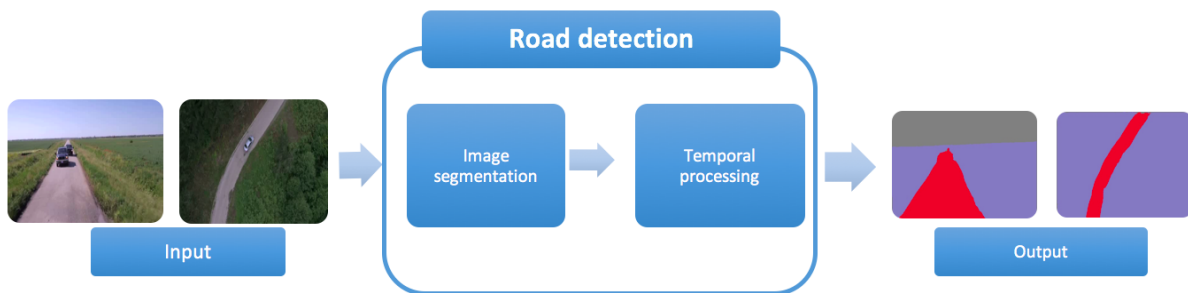


Figure 1: Block diagram of the developed system.

2 STATE OF THE ART

Getting a computer to recognize a road in an image is a great challenge. There is a wide variety of surroundings where a road can be located. This forces to create a quite generic detector in order to obtain good results in diverse locations, where the colors and illumination of the road may greatly vary in different scenes. The first road detectors that were developed focused on well paved roads with clear edges. In this case, it was relatively easy to find the limits of the road or even road marks, using techniques like the Hough transformation (Southall and Taylor, 2001) (Yu and Jain, 1997) or color-based segmentation (Sun et al., 2006) (Chiu and Lin, 2005) (He et al., 2004). However, these approaches allow for little variation in the type of road that can be detected. The Hough transform will have a poor performance in dirt roads and rural areas, where it is more likely to find bushes and sand covering the limit lines and, therefore, complicating its detection. In turn, the main problem for the color-based techniques will be the broad diversity of colors that can present a road depending on the illumination, material and conditions of the road. Moreover, other objects with a similar color to the road will be often found in the scene, giving rise to false positives.

Recently, some more research has been done in this field, specially to apply it on self-driving cars. Although good results were obtained with techniques like Support Vector Machines (SVM) (Zhou et al., 2010) or model-based object detectors (Felzenszwalb et al., 2010), a great improvement was made with the popularization of Convolutional Neural Networks (CNN) after the appearance of the AlexNet (Krizhevsky et al., 2012). Owing to their great performance, CNNs are now one of the preferred solutions for image recognition. One of the recently developed CNN-based systems is SegNet (Badrinarayanan et al., 2015), used in this paper.

The vast majority of studies focus on a driver’s viewpoint, but this approach is very different from

the one we seek in this work, where the images are captured by a drone with an aerial view of the road. Although there exist some approaches to road detection from an aerial viewpoint, they are based on classical methods such as snakes (Laptev et al., 2000), histogram based thresholding and lines detection using the Hough transform (Lin and Saripalli, 2012) or homography-alignment-based tracking and graph cuts detection (Zhou et al., 2015). The main contributions of this paper are to extend the current approaches of road segmentation to aerial imagery using convolutional neural networks and to provide a database to do so, as well as a tool for automatically labeling a video sequence using only the manual segmentation of the first frame.

3 ROAD DETECTION

3.1 Image Segmentation

The first step of the proposed method is to segment all the frames of a video into different classes, in our case *road*, *sky* and *other*. To do so, we use SegNet, a deep convolutional encoder-decoder architecture with a final pixel-wise classification layer, capable of segmenting an image in various classes in real time. This system achieves state-of-the-art performance and is trained to recognize road scenes, which makes it a good starting point for our purpose. However, we need to slightly modify it to fit our interests better.

One of the parameters to modify is the frequency of appearance of each class. This is used for class balancing, which improves the results when the number of pixels belonging to a class is much lesser than another (in our case, the classes *road* and *sky* are far less abundant than the class *other*). The frequency of appearance is used to weight each class in the neural network’s error function, so a mistake in the classification of a pixel belonging to a less frequent class will be more penalized. As our database and classes are different from the SegNet original’s, the provided

class frequencies are not coherent with the images used. In order to compute our own class frequencies, we use the same equation as the SegNet authors,

$$\alpha_c = \text{median_freq} / \text{freq}(c)$$

where $\text{freq}(c)$ is the number of pixels in class c divided by the number of pixels that belong to an image where class c appears, and median_freq is the median of those frequencies.

On another note, as we use a brand new database that we had to label, we decided to only use 3 classes. However, in section 5 we will see that we do not train the neural network from scratch, we fine-tune it in order to take advantage of the information learned in its original training. This is done by initializing the neural network with some pretrained weights and then training it with the new database. The pretrained weights we have used are the ones corresponding to the final model of SegNet. Therefore, the layers of the network are initially configured to segment an image in 11 classes. In order to deal with the change on the number of classes, we set the class frequencies of the remaining 8 classes to 0 in the Softmax layer of the neural network, where the class balancing is done.

With these changes, SegNet is modified to fit our purpose. Figure 2 shows the final appearance of the image segmentation block. SegNet now provides 3 probability images, one for each class. In each of these images, every pixel is set with its probability of belonging to the corresponding class. This is done for all the frames in a video and the resulting probabilities are then passed onto the temporal processing block.

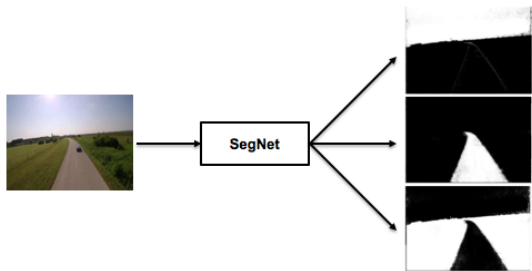


Figure 2: Input and output of SegNet. The output shows a probability images for each class (*sky*, *road* and *other* in this order). The whiter the pixel, the more probable that it belongs to the corresponding class.

3.2 Temporal Processing

In order to make the most of the temporal characteristics of the videos, we have added an additional processing block after SegNet’s segmentation. We take

advantage of the temporal continuity of the videos, as they do not have abrupt changes in the scene from frame to frame. Therefore, we can do an image rectification between a frame and its consecutive with a minimal error. There exist two main methods to align two frames. On the one hand, one can look for *interesting* points (mostly corners) in one of the images and try to find those same points in the other frame. Then, the movement of these points from one frame to the other is calculated, and one of the frames is transformed to counterbalance the motion of the camera. On the other hand, it is possible to align two frames taking into account the whole image and not only some points. This is the method we use, as the *interesting* points in our images would mostly belong to moving vehicles. Therefore, if we took those points as a reference, we would counterbalance the whole scene based on the movement of a vehicle, not the motion of the camera. In order to estimate the transformation that has to be applied to one of the frames to align them, we use the Enhanced Correlation Coefficient (ECC) algorithm (Evdangelidis and Psarakis, 2008). This iterative algorithm provides the transformation that maximizes the correlation coefficient (1) between the first frame (i_r) and the second one after it is transformed (i_w) with transformation parameters \mathbf{p} .

$$\rho(\mathbf{p}) = \frac{\overline{i_r i_w(\mathbf{p})}}{\|i_r\| \|i_w(\mathbf{p})\|} \quad (1)$$

Once we have found the optimum transformation we can align both frames and, therefore, know which pixel on the first frame corresponds to one on the second frame (although some of them will remain unpaired). With this, we can add the probabilities of a pixel throughout a sequence of images in a video, thus obtaining a cumulative probability for each class. When classifying a pixel of a frame, we will choose the class with the highest cumulative probability, taking into account the last 10 frames. The results obtained with this additional processing are more robust and coherent in time. The detail on the results can be found in section 5.

4 DATABASE

Due to the main component of our road detector being a neural network, we need to carry out a training phase prior to obtaining a good performance. However, the training of a neural network requires a labelled database. As we could not find a suitable one for our work nor had the resources to create enough material of our own, we gathered unlabelled videos from different sources and labelled them ourselves.

This database¹ consists of 3.323 images from 22 different scenes. All the images have been captured by a flying drone and the main element in the scene is a road, but the illumination and viewpoint varies greatly in each video (Figure 3). The surroundings are also varied, although most of them are rural.



Figure 3: Some examples of images in the drones' database.

In order not to manually label thousands of images, we also developed a semi-automatic labelling tool¹ for this purpose, using classical methods instead of deep learning. With this tool it is only necessary to manually label the first frame of each video, and the algorithm will adequately propagate these labels to the rest of the sequence. If there was an abrupt change in a scene, a frame in the middle of the video sequence can also be manually labelled in order to resume the propagation to the rest of the sequence taking those labels as the initial point. The steps of the developed algorithm are the following:

1. Manually define a marker for each desired region (*road*, *sky* and *other* in our case) on the first frame of a video and apply the watershed algorithm to obtain a segmented image (Figure 4).



Figure 4: On the left, the first frame of a video sequence, where some seeds or markers have been defined for the *road* (red) and *other* (green) classes. On the right, the segmented image using the watershed technique with the defined markers.

2. Calculate the histogram for each region. Prior to doing so, we convert the RGB image to the HSV color space and keep only the first channel (Hue).

¹<https://imatge.upc.edu/web/resources/spatio-temporal-road-detection-aerial-imagery-using-cnns-dataset>

3. Do a back projection of the histograms. For every pixel in the image, we determine its probability of belonging to a class by finding the value for its color in the histogram, which we previously normalize (Figure 5).

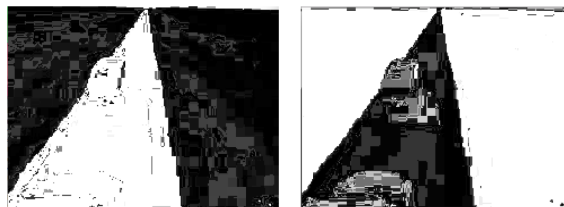


Figure 5: Back projection of the class *road* (left) and *other* (right). They show the probability of each pixel on the image to belong to the corresponding class. The whiter the pixel, the more probable that it belongs to the class.

4. Apply thresholds and a median filter. We adapt the obtained probabilities to watershed markers, dividing them in three groups:
 - If probability = 0: the pixel does not belong to a given class.
 - If $0 < \text{probability} < 0.8$: undefined, it will not count as a marker.
 - If probability > 0.8: the pixel sure belongs to a given class and will be used as a marker on the next frame.

A median filter is also applied, to homogenize the regions of each class. (Figure 6).



Figure 6: Resulting zones after converting the probabilities to markers and homogenizing the regions. For each class, *road* on the left and *other* on the right, there is a safe zone where the pixels sure belong to the corresponding class (white), a fuzzy zone where no markers will be defined (gray) and an unsafe zone that indicates the pixels that do not belong to the class (black).

5. Eliminate the markers on the edges. The limits among watershed regions can be located and dilated, creating a fuzzy zone between regions, where no watershed marker will be set. This way, the contour of the regions in an image will be determined by the watershed algorithm, instead of the markers of the previous frame.
6. Eliminate conflicting markers. A marker for a given class can only be located in an area that be-

longed to that same class in the previous frame. Thus, a region will only expand to adjacent zones and sporadic markers will be avoided. As a counterpoint, new elements in an image won't be detected if they are not in contact with a labelled element of the same class. However, this is not often a big issue in the kind of videos used for this paper, as there are no abrupt changes in the scenes. In any case, a mid-sequence frame can also be manually labelled according to the desired regions and propagate the labels from that point in the video.

7. Apply the watershed algorithm in the next frame using the defined markers and go back to step 2 (Figure 7).



Figure 7: On the left, the resulting markers where red belongs to the class *road*, green belongs to the class *other* and blue determines the undefined regions. On the right, the segmented image after applying the watershed technique on the second frame (image on the center) using the markers obtained.

Some examples of the segmentation obtained with the developed system are shown in Figure 8. We can only do a subjective evaluation of these results, as we do not have any ground truth to compare the results with. In fact, this segmentation will be used as the ground truth from now on. As for the developed method, the results are fairly good and it has a fast execution time, almost in real time. Even though the labels of the first frame have to be manually defined, this also gives the user a chance to define the desired classes. As a counterpoint, if the markers of a certain region disappear at any moment, it will not be possible to automatically recover them. However, the process can be stopped and then resumed taking any frame of the video as the initial point, with a redefinition of the markers.

Once the database is labelled, we can train the neural network. In order to prevent overfitting, the database is divided in three sets: train, validation and test. The first one is used to train the neural network and then the results are evaluated with the validation set. Finally, the neural network is evaluated with the test set to check that it delivers a good performance for images that were not used in the training process. If the neural network is not overfitted, the results obtained with the three sets should be similar. The details on the trainings we carried out can be found in the next section.

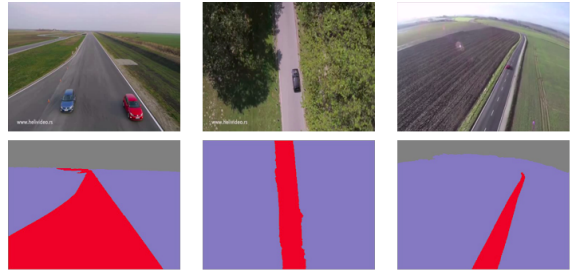


Figure 8: In the first row, some images of the drones' database. In the second row, their corresponding labels obtained with the developed labelling tool.

5 EXPERIMENTAL RESULTS

5.1 Image Segmentation

In order to evaluate the results obtained with the different trainings of SegNet we use the same method as the authors of this architecture, calculating the percentage of well classified pixels in each image. The set of images for the test consists of 1.199 frames of several videos recorded by drones.

The SegNet was initially trained for segmenting images captured from a driver's point of view. For that reason, it does not recognize the different objects in our set of images, as the viewpoint is very different. In Figure 9 there is an example of the segmentation obtained when using the original SegNet in images of the database that was used for its training, the CamVid data set. The segmentation of these images is very good and takes into account SegNet's original 11 classes.

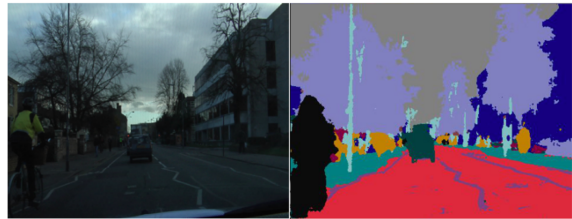


Figure 9: Image of the CamVid database, segmented with the original SegNet.

If we use the same original configuration of SegNet to classify images of the database used in this paper, the results are considerably worse. In Figure 10 we can see how some plants and trees are classified as trees (sky blue), but the rest of the classes are not correctly detected. Even if we regrouped the 11 classes in only 3 (*sky*, *road* and *others*), the classification would still be terrible.

Given these bad results, we proceeded to retrain the our modified version of SegNet with the database



Figure 10: Image on the drones’ database, segmented with the original SegNet. Gray belongs to the sky, green to vehicles, yellow to pedestrians, dark blue to buildings, sky blue to trees, maroon to road and red to pavement.

detailed in section 4. The first experiment was to train the SegNet from scratch. We trained two versions with this database, one with class balancing and one without. The results in Table 1 indicate that the training without class balancing provides better global results. However, the sky and road are better classified when we use class balancing, as they are minority classes that benefit from class balancing.

Table 1: Evaluation of SegNet trained from scratch with this paper’s database.

Precision (%)	<i>Sky</i>	<i>Road</i>	<i>Other</i>	Global
No class balancing	76.59	70.61	95.03	85.60
Class balancing	77.71	71.54	91.07	83.80

These results are clearly improvable so, in order to take advantage of the information generated in SegNet’s original training - which provides very good results as seen in Figure 9 -, we fine-tuned our neural network instead of retraining it from scratch. We used SegNet’s final model, trained with 3.5K images as mentioned in the previous section, and fine-tuned it with the drones’ database. The results of this training are in Table 2, and show a big improvement in relation to training the neural network from scratch.

Table 2: Evaluation of the original SegNet fine-tuned with this paper’s database, without the temporal processing block.

Precision (%)	<i>Sky</i>	<i>Road</i>	<i>Other</i>	Global
No class balancing	99.48	84.52	95.06	91.82
Class balancing	99.70	93.18	91.53	93.13

In the projects that deal with images is equally, if not more, important to evaluate the results subjectively than objectively. In Figure 11 we can see a big improvement in contour definition when fine-tuning instead of training from scratch. Moreover, we can observe how including class balancing provides more homogeneous classes, as some random groups

of badly classified pixels disappear.

5.2 Temporal Processing

When adding a temporal processing block after SegNet’s pixel-wise classification, isolated badly classified pixels are corrected. The classes become more homogeneous and the classification is more robust over time. In order to decide the number of frames to take into account and the maximum iterations of the ECC algorithm, we perform several tests, using our fine-tuned version of SegNet, with class balancing. Table 3 shows the results obtained when varying the maximum number of iterations allowed on the ECC iterative algorithm.

Table 3: Evaluation of the temporal processing block’s performance depending on the number of maximum iterations allowed on the ECC iterative algorithm.

Precision (%)	<i>Sky</i>	<i>Road</i>	<i>Other</i>	Global
10 frames 5 iterations	99.62	94.21	92.45	93.98
10 frames 100 iterations	99.62	94.24	92.44	93.97

Both objective and subjective results are almost identical for 5 or 100 iterations in the ECC algorithm, but the latest causes a big delay in the execution time of the system. Thus, as the results are very similar but one of the options is considerably faster than the other, we set 5 as the maximum iterations allowed in the ECC algorithm for image alignment. With the iterations set to 5, we modify the number of past frames to take into account when processing the current frame. The best result, both objectively and subjectively, is obtained when taking into account the last 10 frames (Table 4) and using 5 iterations for the ECC algorithm, which is our final configuration of the system.

Table 4: Evaluation of the temporal processing block’s performance depending on the number of past frames taken into account. For each evaluation, the precision and recall values are provided, in %.

Precision/Recall	<i>Sky</i>	<i>Road</i>	<i>Other</i>	Global
5 frames, 5 iterations	98.97	92.56	89.90	91.31
10 frames, 5 iterations	99.62	94.24	92.44	93.97
15 frames, 5 iterations	98.42	75.28	91.62	92.35
20 frames, 5 iterations	89.77	91.01	95.14	91.97

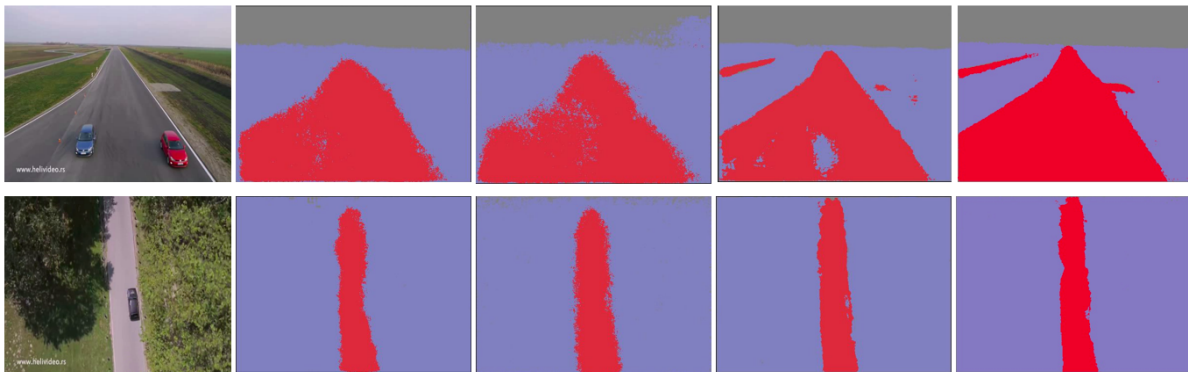


Figure 11: Comparison of the results obtained with different trainings of SegNet. In the first column, the input image. In the second and third column, the result obtained after training SegNet from scratch, without and with class balancing. In the last two columns, the result obtained after fine-tuning SegNet, without and with class balancing.

The modification of these parameters do not cause a huge difference, so we have omitted the visual results of each of the tests. However, Figure 12 presents the comparison between the result obtained at the end of the neural network and the one obtained after the temporal processing, although the improvement is not as notable in a few images as in a video sequence.

6 CONCLUSIONS

Applying computer vision on drones is a very new and extensive field that will give raise to many new developments in the following years. In turn, road detection will play an important role in these applications, as drones are mostly used in outside locations, where roads are almost always present. Therefore, in the vast majority of new developments involving drones, roads will probably be either the object of study or used as a reference for location.

Defining a generic road and vehicle detector is complex, specially due to the big variety of input images. If it was defined that the imagery would always be captured from the same point of view or that the conditions of the road and surroundings would always be similar, the adjustment of some parameters in the detector would enhance the results. However, the challenge of this paper was to develop a very generic detector that would work in very diverse surroundings.

In this work, we extend the most popular approach to road detection, which is working on images from a driver's viewpoint, to aerial imagery. We prove with our experimental results that it is possible to detect a road from very diverse aerial points of view with deep learning methods, obtaining an accuracy of over 90%. Moreover, we provide a labelled database of

aerial video sequences where roads are the main object of interest, as well as the semi-automatic tool we have developed to label it.

ACKNOWLEDGMENT

This work has been developed in the framework of projects TEC2013-43935-R and TEC2016-75976-R, financed by the Spanish Ministerio de Economía y Competitividad and the European Regional Development Fund (ERDF).

REFERENCES

- Badrinarayanan, V., Kendall, A., and Cipolla, R. (2015). SegNet: A Deep Convolutional Encoder-Decoder Architecture for Image Segmentation. *CoRR*, abs/1511.0.
- Chiu, K.-Y. and Lin, S.-F. (2005). Lane detection using color-based segmentation. pages 706–711.
- Evangelidis, G. D. and Psarakis, E. Z. (2008). Parametric image alignment using enhanced correlation coefficient maximization. *IEEE Transactions on Pattern Analysis and Machine Intelligence*, 30(10):1858–1865.
- Felzenszwalb, P., Girshick, R., McAllester, D., and Ramanan, D. (2010). Object detection with discriminatively trained part based models. *IEEE Trans. Pattern Analysis and Machine Intelligence*, 32(9):1627–1645.
- He, Y., Wang, H., and Zhang, B. (2004). Color-based road detection in urban traffic scenes. *IEEE Transactions on Intelligent Transportation Systems*, 5(4):309–318.
- Krizhevsky, A., Sutskever, I., and Hinton, G. (2012). Imagenet classification with deep convolutional neural networks. *Proceedings of Neural Information and Processing Systems*.



Figure 12: Comparison of the segmentation obtained with SegNet and the one obtained after the temporal processing.

- Laptev, I., Mayer, H., Lindeberg, T., Eckstein, W., Steger, C., and Baumgartner, A. (2000). Automatic extraction of roads from aerial images based on scale space and snakes. *Machine Vision and Applications*, 12(1):23–31.
- Lin, Y. and Saripalli, S. (2012). Road detection from aerial imagery. In *2012 IEEE International Conference on Robotics and Automation*, pages 3588–3593.
- Southall, B. and Taylor, C. J. (2001). Stochastic road shape estimation. pages 205–212.
- Sun, T.-Y., Tsai, S.-J., and Chan, V. (2006). Hsi color model based lane-marking detection. pages 1168–1172.
- Yu, B. and Jain, A. K. (1997). Lane boundary detection using a multiresolution hough transform. volume 2, pages 748–751.
- Zhou, H., Kong, H., Wei, L., Creighton, D., and Nahavandi, S. (2015). Efficient road detection and tracking for unmanned aerial vehicle. *IEEE Transactions on Intelligent Transportation Systems*, 16(1):297–309.
- Zhou, S., Gong, J., Xiong, G., Chen, H., and Iagnemma, K. (2010). Road detection using support vector machine based on online learning and evaluation. *IEEE Intelligent Vehicles Symposium*, pages 256–261.